

Synthesis and characterization of two one-dimensional lanthanide coordination polymers

Mingcai Yin, Jutang Sun*

Department of Chemistry, Wuhan University, Wuhan 430072, PR China

Received 26 January 2004; received in revised form 12 March 2004; accepted 12 March 2004

Abstract

Two lanthanide coordination polymers $[\text{Eu}(\text{H}_2\text{sal})(\text{Hsal})(\text{sal})\cdot\text{H}_2\text{O}]_n$ (**1**) and $\{[\text{Tb}(\text{FUR})_3(\text{H}_2\text{O})_2]\cdot\text{DMF}\}_n$ (**2**) (H_2sal , salicylic acid; Hsal^- , $o\text{-HOC}_6\text{H}_4\text{CO}_2^-$; HFUR , α -furancarboxylic acid; DMF , N,N -dimethylformamide) were synthesized and characterized by elemental analysis, TG, IR, and luminescence spectra. The crystal structures were determined by X-ray single crystal analysis. Both complexes are one-dimensional polymers. Probably the luminescence quenching of complex **1** is assigned to its special one-dimensional ribbon structure. The vibration energy level caused by the one-dimensional ribbon and located between $^5\text{D}_0$ and $^7\text{F}_j$ maybe is the main reason. Complex **2** displays intense green luminescence under the excitation of UV light. The emission bands at 486, 541, 584, and 618 nm are attributed to the characteristic $^5\text{D}_4 \rightarrow ^7\text{F}_j$ ($j = 6, 5, 4, 3$) transitions of Tb(III) ions, respectively.

© 2004 Elsevier B.V. All rights reserved.

Keywords: Coordination polymer; Lanthanide complexes; Crystal structure; Luminescence

1. Introduction

Nowadays great attention has been paid to the lanthanide aromatic carboxylates owing to its novel structures and potential applications in material sciences such as supraconductor, magnetic materials, and luminescent probes [1–5]. Up to now, many lanthanide aromatic carboxylates have been reported, which are commonly in dimeric or polymeric forms [6–12]. As a part of our studies on the structure and luminescence of lanthanide aromatic carboxylates, two one-dimensional coordination polymers $[\text{Eu}(\text{H}_2\text{sal})(\text{Hsal})(\text{sal})\cdot\text{H}_2\text{O}]_n$ (**1**) and $\{[\text{Tb}(\text{FUR})_3(\text{H}_2\text{O})_2]\cdot\text{DMF}\}_n$ (**2**) (H_2sal , salicylic acid; Hsal^- , $o\text{-HOC}_6\text{H}_4\text{CO}_2^-$; HFUR , α -furancarboxylic acid; DMF , N,N -dimethylformamide) were obtained. The structures and luminescence properties are reported here.

2. Experimental

2.1. Materials and methods

$\text{EuCl}_3\cdot 5\text{H}_2\text{O}$ and $\text{Tb}_2(\text{CO}_3)_3$ were prepared in our laboratory. All other chemicals were analytical reagent grade. The IR spectra were recorded on a Thermo Nicolet Avatar 360 FT-IR spectrophotometer using KBr pellets. Elemental analyses were carried out with a Perkin-Elmer 240B elemental analyzer. The thermogravimetric analyses were conducted on a Shimadzu DT-40 thermal analyzer at a heating rate of $20^\circ\text{C}/\text{min}$ in air. The X-ray powder diffractions were performed on a Shimadzu XRD-6000 powder diffractionmeter. The excitation and emission spectra of the solid sample were measured on a Shimadzu RF-5301PC spectrofluorophotometer at room temperature.

2.2. Synthesis of $[\text{Eu}(\text{H}_2\text{sal})(\text{Hsal})(\text{sal})\cdot\text{H}_2\text{O}]_n$ (**1**)

An aqueous solution of $\text{EuCl}_3\cdot 5\text{H}_2\text{O}$ (0.35 g, 1.0 mmol) was added dropwise to an aqueous solution of $\text{Na}[o\text{-HOC}_6\text{H}_4\text{CO}_2]$ (0.50 g, 3.0 mmol) under stirring and light-yellow precipitants were formed immediately. The mixture was stirred for about 10 min at room temperature and filtered.

* Corresponding author. Tel.: +86-27-87218494; fax: +86-27-87647617.

E-mail address: jtsun@whu.edu.cn (J. Sun).

Table 1
Crystal data and structure refinement for **1**

Compound	1	2
Empirical formula	C ₂₁ H ₁₇ EuO ₁₀	C ₁₈ H ₂₀ NO ₁₂ Tb
Formula weight	581.31	601.27
Temperature (K)	291(2)	293(2)
Wavelength (Å)	0.71073	0.71073
Crystal system, space group	Monoclinic, <i>p</i> 2 ₁ / <i>n</i>	Triclinic, <i>p</i> 1
<i>a</i> (Å)	13.633(3)	9.786(2)
<i>b</i> (Å)	6.7476(13)	11.122(2)
<i>c</i> (Å)	22.730(5)	11.259(2)
α (°)	90	76.81(3)
β (°)	100.06(3)	69.81(3)
γ (°)	90	75.72(3)
<i>V</i> (Å ³)	2058.8(7)	1100.8(4)
<i>Z</i> , <i>D</i> _{calculated} (g/cm ³)	4, 1.875	2, 1.814
μ (mm ⁻¹)	3.104	3.276
<i>F</i> (000)	1144	592
Crystal size (mm)	0.20 × 0.20 × 0.18	0.20 × 0.18 × 0.18
θ range for data collection (°)	1.63–27.54	1.91–27.51
Index ranges	0 ≤ <i>h</i> ≤ 17, −8 ≤ <i>k</i> ≤ 8, −29 ≤ <i>l</i> ≤ 29	−12 ≤ <i>h</i> ≤ 11, −14 ≤ <i>k</i> ≤ 0, −14 ≤ <i>l</i> ≤ 13
Reflections collected/unique	7712/4429	4386/4386
Completeness to max θ (%)	93.3	88.49
Maximum and minimum transmission	0.6050 and 0.5756	0.6146 and 0.6146
Refinement method	Full matrix least squares on <i>F</i> ²	Full matrix least squares on <i>F</i> ²
Data/restraints/parameters	4429/0/290	4386/0/290
Goodness-of-fit on <i>F</i> ²	1.158	1.212
Final <i>R</i> indices [<i>I</i> > 2σ(<i>I</i>)] (<i>R</i> 1, <i>wR</i> 2)	0.0402, 0.1117	0.0369, 0.1039
<i>R</i> indices (all data) (<i>R</i> 1, <i>wR</i> 2)	0.0493, 0.1152	0.0411, 0.1068
Extinction coefficient	0.0046(4)	0.0373(17)
Largest diff. peak and hole (e/Å ³)	1.588 and −1.477	1.128 and −1.519

Light-yellow needle-like crystals were obtained from the filtrate after about 2 weeks (0.15 g in the yield of 25.86%). Elemental analysis for C₂₁H₁₇EuO₁₀ (%): found (calc.): C 43.18 (43.38), H 3.01 (2.93). IR (KBr, cm⁻¹): 3439.0 (m), 1623.9 (s), 1594.8.1 (s), 1565.3 (vs), 1548.7 (vs), 1512.0 (m), 1482.8 (s), 1465.0 (vs), 1426.4 (vs), 1387.6 (vs), 1307.1 (m), 1248.1 (m), 1216.3 (m), 1147.3 (m), 1032.7 (m), 883.3 (m), 852.5 (m), 806.2 (m), 756.0 (s), 704.0 (m), 663.5 (m), 572.8 (w), 528.5 (w), 484.1 (w), and 472.5 (m).

2.3. Synthesis of {[Tb(FUR)₃(H₂O)₂]·DMF}_n (**2**)

SrCl₂·6H₂O (0.26 g, 1.0 mmol), 0.24 g (0.5 mmol) Tb₂(CO₃)₃, 0.58 g (5.0 mmol) α-furancarboxylic acid, and 2.9 ml distilled water were mixed in a Teflon-lined stainless steel container to get a rheological phase. The container was sealed and reacted at 90 °C for 3 days. The white powders obtained were dissolved in a H₂O/DMF (9:1) solvent and evaporated at room temperature. Colorless prismatic crystals were formed after several days [0.25 g in the yield of 41.7% based on Tb₂(CO₃)₃]. Elemental analysis for C₁₈H₂₀NO₁₂Tb (%): found (calc.): C 35.78 (35.92), H 3.21 (3.33), N 2.35 (2.33). IR (KBr, cm⁻¹): 3134.1 (s), 1589.2 (vs), 1558.4 (vs), 1541.0 (vs), 1481.2 (vs), 1419.5 (vs), 1398.3 (vs), 1373.2 (vs), 1228.6 (m), 1199.6 (w), 1141.8 (w), 1078.1 (m), 1014.5 (m), 785.0 (s), 758.0 (m), 613.3 (w), 555.5 (w), and 470.6 (m).

2.4. Crystallographic measurement and structure resolution

The X-ray crystallography data for complexes **1** and **2** were collected on a RIGAKU R-AXIS IV imaging plate diffractionmeter with graphite-monochromated Mo Kα radiation ($\lambda = 0.71073$ Å). The structures were solved by direct methods and refined by full matrix least squares on *F*² using the SHELXL-97 and SHELXS-97 programs [13], respectively. All non-hydrogen atoms were refined with anisotropic displacement parameters. The hydrogen atoms were generated geometrically and treated by a mixture of independent and constrained refinements. A summary of crystallographic data and refinement details is given in Table 1. Selected bond lengths and angles for **1** and **2** are listed in Tables 2 and 3, respectively.

3. Results and discussion

3.1. IR spectra

The IR spectra of salicylic acid, α-furancarboxylic acid, and both complexes were determined over the range 4000–400 cm⁻¹ using KBr pellets and the spectra of complexes **1** and **2** in the range of 2000–400 cm⁻¹ are shown in Fig. 1. The absorption bands of M–O bond appear at 484.1

Table 2
Selected bond lengths (Å) and bond angles (°) for complex **1**

Bond	Length	Bond	Length
Eu(1)–O(6)	2.353(4)	Eu(1)–O(8)#1	2.500(3)
Eu(1)–O(10)	2.410(4)	Eu(1)–O(7)	2.546(3)
Eu(1)–O(5)#1	2.427(4)	Eu(1)–O(8)	2.585(3)
Eu(1)–O(9)#2	2.431(3)	Eu(1)–Eu(1)#1	4.2135(7)
Eu(1)–O(7)#2	2.470(4)	Eu(1)–Eu(1)#2	4.2135(7)
Eu(1)–O(3)	2.478(4)		
Bond	Angle	Bond	Angle
O(2)–C(7)–O(3)	121.3(5)	Eu(1)#1–O(7)–Eu(1)	114.26(12)
O(5)–C(14)–O(6)	123.2(5)	O(6)–Eu(1)–O(3)	123.06(14)
O(7)–C(21)–O(8)	117.5(4)	O(10)–Eu(1)–O(3)	75.85(14)
O(10)–Eu(1)–O(5)#1	67.23(13)	O(5)#1–Eu(1)–O(3)	71.13(13)
O(6)–Eu(1)–O(9)#2	79.55(13)	O(9)#2–Eu(1)–O(3)	69.51(12)
O(10)–Eu(1)–O(9)#2	83.98(14)	O(7)#2–Eu(1)–O(3)	126.92(11)
O(5)#1–Eu(1)–O(9)#2	135.66(12)	O(6)–Eu(1)–O(8)#1	71.12(12)
O(6)–Eu(1)–O(7)#2	75.04(13)	O(10)–Eu(1)–O(8)#1	141.20(12)
O(10)–Eu(1)–O(7)#2	72.35(13)	O(5)#1–Eu(1)–O(8)#1	81.18(12)
O(5)#1–Eu(1)–O(7)#2	128.83(12)	O(8)#1–Eu(1)–O(7)	64.30(11)
O(9)#2–Eu(1)–O(8)#1	105.60(12)	O(6)–Eu(1)–O(8)	85.42(13)
O(7)#2–Eu(1)–O(8)#1	146.12(12)	O(10)–Eu(1)–O(8)	83.72(13)
O(3)–Eu(1)–O(8)#1	72.92(12)	O(5)#1–Eu(1)–O(8)	81.23(12)
O(6)–Eu(1)–O(7)	74.52(13)	O(9)#2–Eu(1)–O(8)	129.96(12)
O(10)–Eu(1)–O(7)	119.37(13)	O(7)#2–Eu(1)–O(8)	64.14(10)
O(5)#1–Eu(1)–O(7)	68.74(12)	O(3)–Eu(1)–O(8)	150.30(13)
O(9)#2–Eu(1)–O(7)	154.01(13)	O(8)#1–Eu(1)–O(8)	114.02(7)
O(7)#2–Eu(1)–O(7)	108.18(9)	O(7)–Eu(1)–O(8)	50.02(11)
O(3)–Eu(1)–O(7)	124.36(12)	Eu(1)#1–O(7)–Eu(1)	114.26(12)
O(9)#2–Eu(1)–O(7)#2	65.89(11)	Eu(1)#2–O(8)–Eu(1)	111.92(12)
Eu(1)#2–O(8)–Eu(1)	111.92(12)		

Table 3
Selected bond lengths (Å) and bond angles (°) for complex **2**

Bond	Length	Bond	Length
Tb(1)–O(7)#1	2.282(4)	Tb(1)–O(10)	2.469(5)
Tb(1)–O(2)#2	2.295(5)	Tb(1)–O(4)	2.491(5)
Tb(1)–O(8)	2.327(4)	Tb(1)–O(5)	2.495(5)
Tb(1)–O(1)	2.346(4)	O(2)–Tb(1)#2	2.295(5)
Tb(1)–O(11)	2.453(4)	O(7)–Tb(1)#1	2.282(4)
Bond	Angle	Bond	Angle
O(2)–C(1)–O(1)	124.9(5)	O(1)–Tb(1)–O(10)	81.39(16)
O(4)–C(6)–O(5)	121.5(6)	O(11)–Tb(1)–O(10)	71.21(16)
O(8)–C(11)–O(7)	124.7(5)	O(7)#1–Tb(1)–O(4)	78.61(16)
O(7)#1–Tb(1)–O(8)	102.68(16)	O(2)#2–Tb(1)–O(4)	74.04(16)
O(2)#2–Tb(1)–O(8)	83.68(17)	O(8)–Tb(1)–O(4)	128.61(17)
O(7)#1–Tb(1)–O(1)	82.83(16)	O(1)–Tb(1)–O(4)	77.56(16)
O(2)#2–Tb(1)–O(1)	104.94(16)	O(11)–Tb(1)–O(4)	130.15(14)
O(8)–Tb(1)–O(1)	153.75(19)	O(10)–Tb(1)–O(4)	144.63(16)
O(7)#1–Tb(1)–O(11)	139.46(18)	O(7)#1–Tb(1)–O(5)	73.28(17)
O(2)#2–Tb(1)–O(11)	71.21(17)	O(2)#2–Tb(1)–O(5)	78.53(17)
O(8)–Tb(1)–O(11)	81.47(16)	O(8)–Tb(1)–O(5)	78.24(17)
O(1)–Tb(1)–O(11)	78.15(16)	O(1)–Tb(1)–O(5)	127.46(16)
O(7)#1–Tb(1)–O(10)	70.77(17)	O(11)–Tb(1)–O(5)	145.09(16)
O(2)#2–Tb(1)–O(10)	139.53(17)	O(10)–Tb(1)–O(5)	129.54(15)
O(8)–Tb(1)–O(10)	76.47(17)	O(4)–Tb(1)–O(5)	52.50(14)

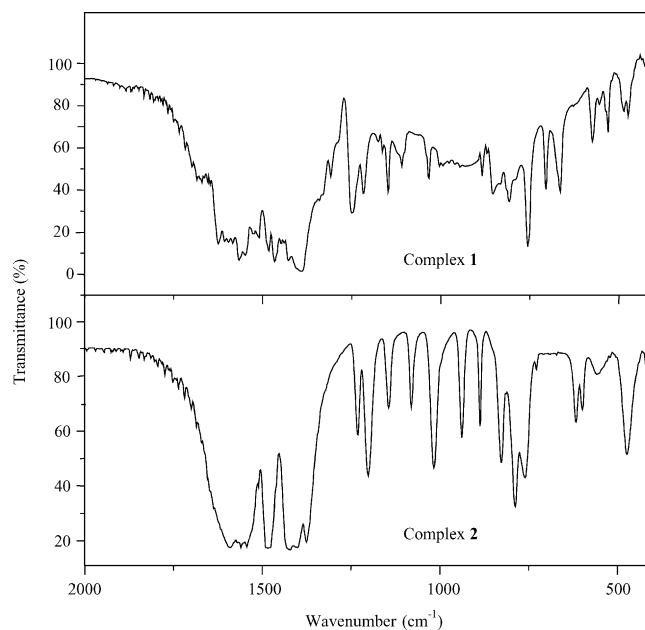


Fig. 1. The IR spectra of complexes **1** and **2**.

and 472.5 cm^{-1} for **1** and 470.6 cm^{-1} for **2**. The absence of band in the region $1690\text{--}1730\text{ cm}^{-1}$ for **2** indicates the complete deprotonation of the COOH groups. The asymmetric and symmetric stretching vibration bands of CO_2^- groups appear at 1565.3 , 1548.7 , 1426.4 , and 1387.6 cm^{-1} for **1** and 1558.4 , 1541.0 , 1419.5 , 1398.3 , and 1373.2 cm^{-1} for **2**, respectively, which indicates that the CO_2^- groups function in different coordination modes. The strong absorption band which occurred at 1482.8 cm^{-1} indicates the existence of uncoordinated phenolic hydroxyl group in complex **1**, consisting with the results of X-ray analyses in the next section.

3.2. Structure description

3.2.1. Structure of $[\text{Eu}(\text{H}_2\text{sal})(\text{Hsal})(\text{sal})\cdot\text{H}_2\text{O}]_n$ (**1**)

The structure of complex **1** is shown in Fig. 2. It is in a low symmetry and there is no discrete europium salicylate molecule in the crystal. It can be seen that the salicylate ligands are in three coordination modes, namely (a) monodentate salicylic acid molecule through its carbonyl oxygen atom, (b) bidentate bridging salicylate group through two carboxyl oxygen atoms, and (c) pentadentate chelating-bridging salicylate group through both the carboxyl and the phenolic oxygen atoms (as shown in Fig. 3), the same as those in the lanthanide salicylates of Sm, Am, La, and Nd [14].

It is different from the lanthanide salicylates of Tb and Ho [15] but similar to those of Sm and Am [14] that each Eu atom in complex **1** is surrounded by nine oxygen atoms, one from a coordinated water molecule and eight from six salicylate groups, in which one oxygen atom (O3) is in the coordination mode (a), two oxygen atoms

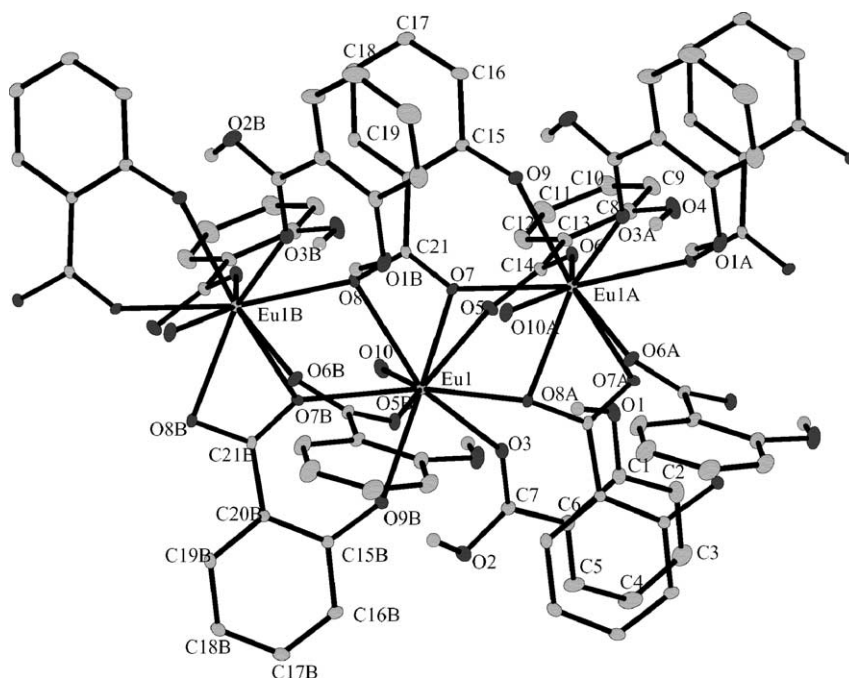


Fig. 2. Molecular structure of complex **1** with 15% thermal ellipsoids.

(O5B, O6) are in the mode (b), and the other five oxygen atoms (O7, O8, O7B, O8A, O9B) are in the mode (c). The Eu–O bonds vary from 2.353 to 2.585 Å and the O–Eu–O angles range from 50.02 to 154.01° (see Table 2 and Fig. 2). The Eu–O bonds of the chelating carboxyl groups (2.546, 2.585 Å) are much longer than that of the bridging carboxyl groups (2.353, 2.427 Å) and the chelating-bridging ones (2.470, 2.500 Å), while the Eu–O bond length of the aqua ligand (2.410 Å) is approximate to that of the phenolic group (2.431 Å). Every two Eu atoms are linked together through three salicylate groups, one in mode (b) and two in mode (c) with a Eu···Eu separation of 4.2135 Å, which results in the formation of one-dimensional ribbon structure [Fig. 4(c)]

through the –Eu–O–C–O–Eu–O–C–O–Eu– [Fig. 4(a)] and the –Eu–O–Eu–O–Eu– [Fig. 4(b)] chains.

In addition to the intramolecular hydrogen bonds formed between the phenolic hydroxyl group and the carboxyl group (O1···O3 = 2.550 Å, O2···O9B = 2.424 Å, and O4···O6 = 2.627 Å), aromatic stacking interactions exist between the phenyl rings containing C8–C13 with the face-to-face distance being ca. 3.62 Å, which link the adjacent one-dimensional ribbons into two-dimensional layers, as displayed in Fig. 5.

3.2.2. Structure of $\{[Tb(FUR)_3(H_2O)_2] \cdot DMF\}_n$ (**2**)

The molecular structure of complex **2** is shown in Fig. 6. Each Tb atom in **2** is eight-coordinated by four oxygen atoms

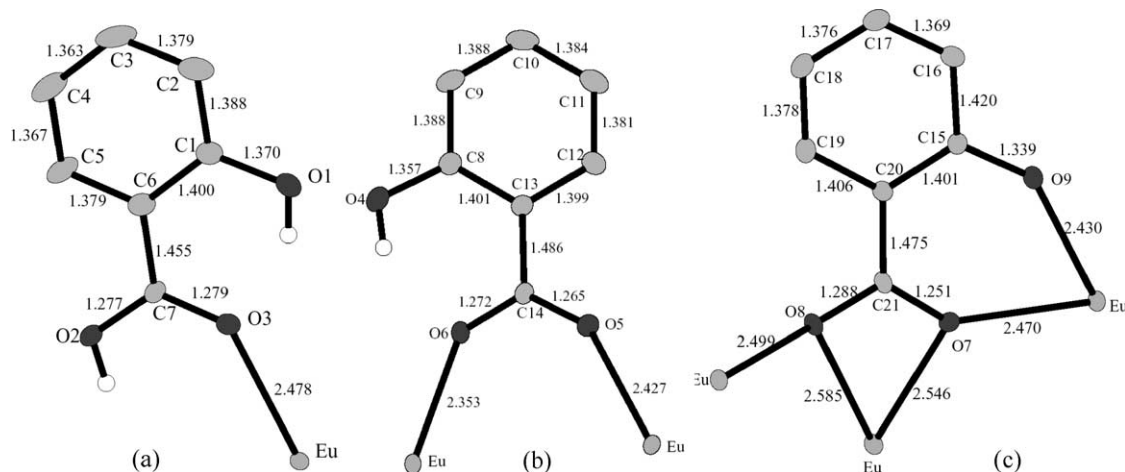


Fig. 3. The coordination modes of salicylate ligand in complex **1**.

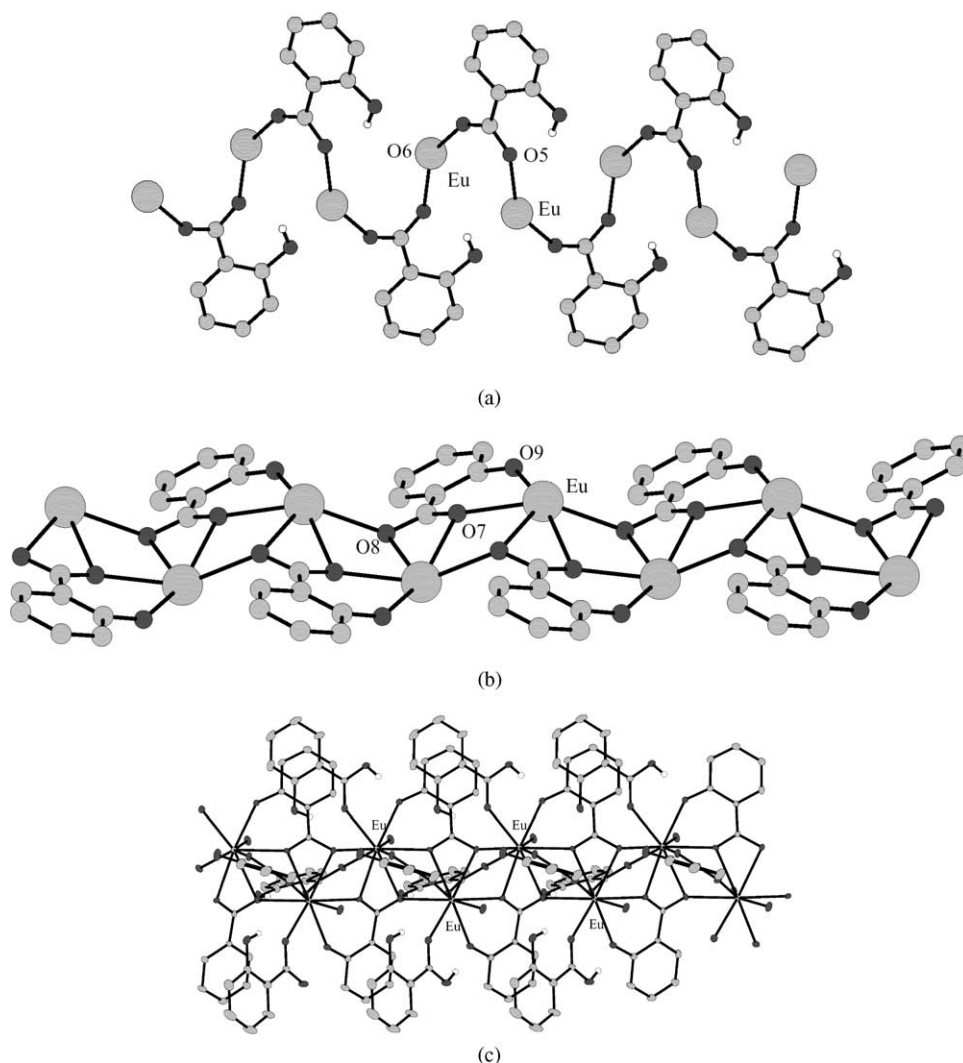


Fig. 4. Stereoscopic view of the (a) $-\text{Eu}-\text{C}-\text{O}-\text{O}-\text{Eu}-\text{O}-\text{C}-\text{O}-\text{Eu}-$ chain, (b) $-\text{Eu}-\text{O}-\text{Eu}-\text{O}-\text{Eu}-$ chain, and (c) one-dimensional ribbon along c -axis in complex **1**.

from four bridging FUR^- groups, two oxygen atoms from one chelating FUR^- group, and two oxygen atoms from two coordinated water molecules, the same as the lanthanide atoms in complexes $\{[\text{Eu}(\text{FUR})_3 \cdot 2\text{H}_2\text{O}] \cdot \text{NO}_3(4,4'\text{-bpy})\}_n$ [7] and $\text{Ln}(o\text{-HOC}_6\text{H}_4\text{CO}_2)_3(\text{H}_2\text{O})_2 \cdot 2\text{H}_2\text{O}$ ($\text{Ln} = \text{Tb}, \text{Ho}$) [15]. The $\text{Tb}-\text{O}$ bonds range from 2.282 to 2.495 Å and the $\text{O}-\text{C}-\text{O}$ angles vary from 121.5 to 124.9°. It is similar to complex **1** that the average $\text{Tb}-\text{O}$ bond of the chelating FUR^- groups (2.493 Å) is a bit longer than that of the bridging ones (2.313 Å) or the water ligands (2.461 Å).

Every two adjacent Tb atoms are linked together by two bridging FUR^- groups, which lead to the formation of a one-dimensional chain, as illustrated in Fig. 7. For the two Tb atoms bridged by the FUR^- groups containing O1 and O2, the $\text{Tb1} \cdots \text{Tb1A}$ separation is 4.882 Å, but for the two Tb atoms bridged by the FUR^- groups containing O7 and O8, the $\text{Tb1} \cdots \text{Tb1B}$ separation is 4.972 Å. The DMF molecules located at both sides of the one-dimensional chain do not coordinated to the Tb

atoms, but hydrogen bonds are formed not only between its carbonyl oxygen atom and the two coordinated water molecules ($\text{O12} \cdots \text{O10A} = 2.75 \text{ \AA}$, $\text{O12} \cdots \text{O11} = 2.76 \text{ \AA}$; Fig. 7), but also between its methyl groups and the furyl oxygen atoms ($\text{C17}-\text{H} \cdots \text{O6} = 2.840 \text{ \AA}$). These hydrogen bonds link the adjacent one-dimensional chains into two-dimensional layers, as displayed in Figs. 7 and 8.

Besides these hydrogen bonds, aromatic stacking interactions exist between the furyl rings of two adjacent chains with the average atom distance being 3.808 Å, which further consolidate the two-dimensional architecture.

3.3. Thermogravimetric analysis (TGA)

The thermal behaviors of complexes **1** and **2** were studied from 30 to 800 °C in air, which agreed with the results of X-ray crystallography. The TG curves showed that the weight loss of complex **1** begins at 166 °C and ends at 655 °C. It decomposes in four steps and the last residue is

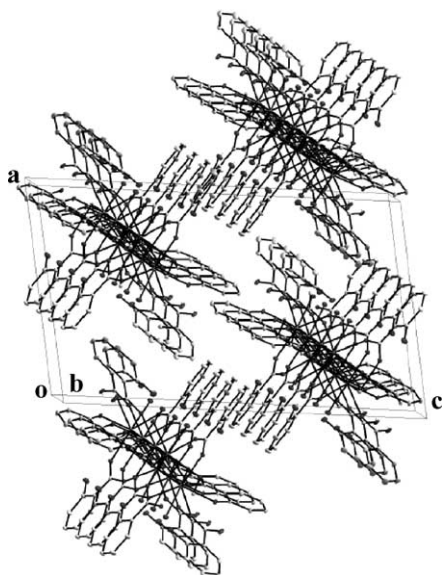


Fig. 5. Packing diagram of complex **1** along *b*-axis.

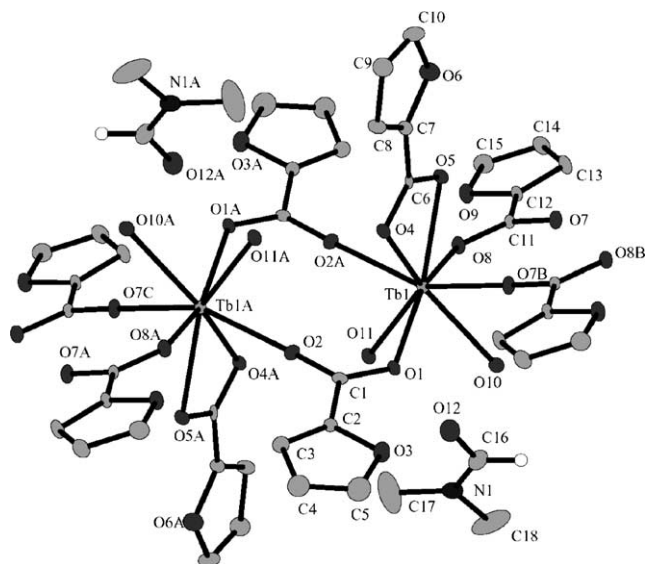


Fig. 6. The coordination environment around Tb atom in complex **2** with 10% probability thermal ellipsoids.

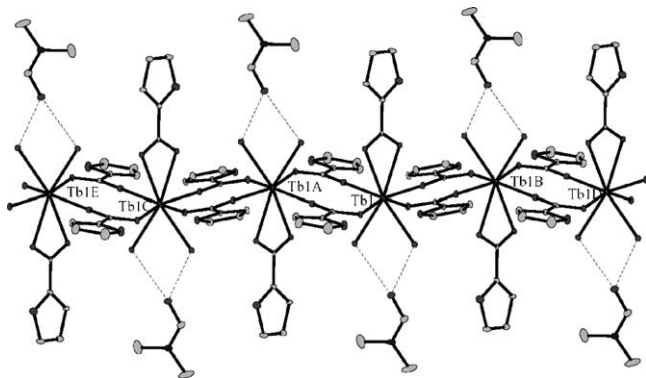


Fig. 7. Stereoscopic view of the one-dimensional chain along *a*-axis in complex **2**.

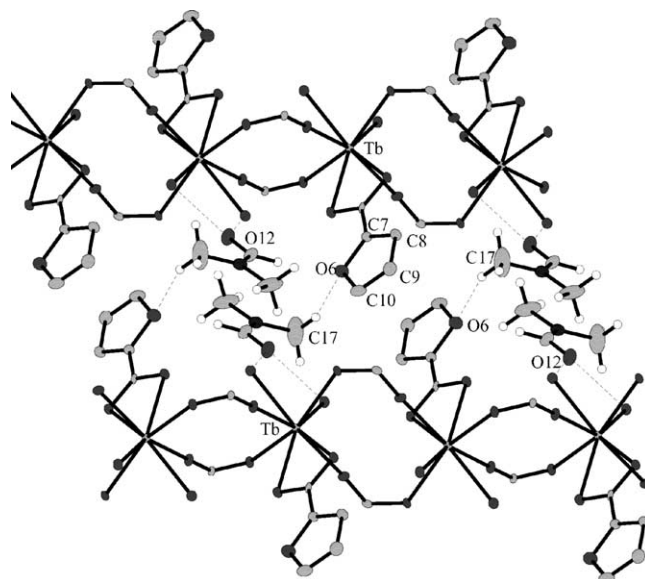


Fig. 8. Stereoscopic view of the hydrogen bonds and the aromatic stacking interactions (some furyl rings are omitted for clarity).

Eu_2O_3 (observed, 30.0%; calculated, 30.26%: in accordance with the JCPDS file 43-1008) [16]. Complex **2** begins to lose weight at 79 °C and the weight loss from 79 to 164.8 °C corresponds to the loss of two coordinated water molecules and one solvent DMF molecule (observed, 16.14%; calculated, 16.09%). The decomposition of the framework begins at 277.1 °C and ends at 643.7 °C. The last residue is Tb_4O_7 (observed, 31.06%; calculated, 31.10%: in agreement with the JCPDS file 32-1286).

3.4. Photoluminescence

3.4.1. Luminescence quenching of complex **1**

It is well known that europium salicylate has no luminescence (both salicylate group and Eu^{3+} ion) when irradiated by UV light, which has been attributed to the energy mismatch between the lowest triplet state of salicylate group and the lowest excited state ($^5\text{D}_0$) of Eu^{3+} ion [17]. However, we think that this explanation is questionable to some extent since if it is right, where is the energy absorbed by the salicylate ligands and how to explain the red luminescence of the ionic dimeric europium salicylate $[\text{Eu}_2(\text{Hsal})_8][\text{Zn}(\text{phen})_3] \cdot (\text{H}_2\text{sal})(\text{H}_2\text{O})$ (phen: 1,10-phenanthroline), in which the phen ligand does not coordinate to Eu^{3+} ions [18]. On the other hand, as far as the energy transfer process, the energy absorbed by the salicylate groups can be transferred to other higher excited state energy levels of Eu^{3+} ion.

Since compound property has close relations to its structure, we attempted to interpret this luminescence quenching from the influence of crystal structure and compared the structure of complex **1** with those of other europium aromatic carboxylates and terbium salicylate [15]. It is found that some differences exist. First, in complex **1**,

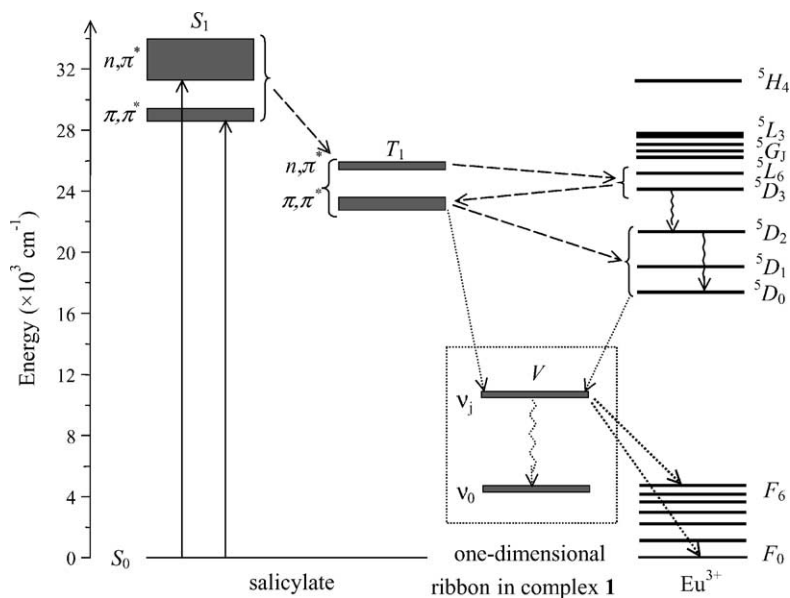


Fig. 9. The possible energy level diagram and energy transfer mechanism for complex 1.

the salicylate group in the coordination mode (c) (Fig. 3) exhibits a better coplanarity than the ligands in the other lanthanide aromatic carboxylates owing to the coordination of phenolic oxygen atoms. In addition, besides the $-\text{Eu}-\text{O}-\text{C}-\text{O}-\text{Eu}-\text{O}-\text{C}-\text{O}-\text{Eu}-$ chains usually occurring in lanthanide aromatic carboxylates, the $-\text{Eu}-\text{O}-\text{Eu}-\text{O}-\text{Eu}-$ chains are also present (Fig. 4), which result in the formation of one-dimensional ribbon structure in complex 1. Compared with the one-dimensional chain in the other lanthanide aromatic carboxylates such as $\text{Eu}(\text{TPA})_3(\text{HTPA})_2$ (HTPA, α -thiophene carboxylic acid), which emits an intense red luminescence when irradiated by UV light [19], the one-dimensional ribbon maybe has a much higher vibration energy level (denoted as V) and probably it is just located between ${}^5\text{D}_0$ and ${}^7\text{F}_j$, which leads to the luminescence quenching or a large red-shift of the luminescence of Eu^{3+} ions so that it exceeds the effective measurement range (220–750 nm; as shown in Fig. 9) [20,21].

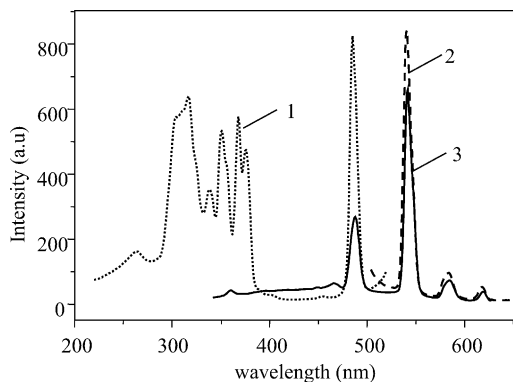


Fig. 10. The solid-state excitation and emission spectra of complex 2 (1, Em = 541 nm; 2, Ex = 485 nm; and 3, Ex = 317 nm).

3.4.2. Luminescence of complex 2

Under the excitation of UV light, complex 2 emits an intense green luminescence. The excitation and emission spectra of the solid sample are shown in Fig. 10. The excitation bands at about 264, 303 nm are assigned to the $n \rightarrow \pi^*$, $\pi \rightarrow \pi^*$ transitions of furoate groups and the sharp peaks located at 317, 338, 351, 368, and 485 nm are attributed to the ${}^7\text{F}_6 \rightarrow {}^5\text{H}_7$, ${}^7\text{F}_6 \rightarrow {}^5\text{L}_6$, ${}^7\text{F}_6 \rightarrow {}^5\text{L}_9$, ${}^7\text{F}_6 \rightarrow {}^5\text{L}_{10}$, and ${}^7\text{F}_6 \rightarrow {}^5\text{D}_4$ transitions of Tb^{3+} ions, respectively. The emission bands at 486, 541, 584, and 618 nm correspond to the characteristic ${}^5\text{D}_4 \rightarrow {}^7\text{F}_j$ ($j = 6, 5, 4, 3$) transitions of Tb^{3+} ions, respectively.

4. Conclusion

Two one-dimensional lanthanide complexes $[\text{Eu}(\text{H}_2\text{sal})\text{-(Hsal)(sal)}\cdot\text{H}_2\text{O}]_n$ (1) and $\{\text{[Tb(FUR)}_3(\text{H}_2\text{O})_2]\cdot\text{DMF}\}_n$ (2) have been synthesized and characterized by X-ray crystallography. The one-dimensional ribbon architecture maybe is the main reason for the luminescence quenching of complex 1. Complex 2 emits an intense green luminescence when excited by UV light.

References

- [1] J.P. Costes, J.M. Clemente-Juan, F. Dahan, F. Nicodme, M. Verelst, *Angew. Chem. Int. Ed.* 41 (2002) 323.
- [2] T.M. Reineke, M. Eddaoudi, M. Fehr, D. Kelly, O.M. Yaghi, *J. Am. Chem. Soc.* 121 (1999) 1651.
- [3] L. Ma, O.R. Evans, B.M. Foxman, W. Lin, *Inorg. Chem.* 38 (1999) 5837.
- [4] J.S. Seo, D. Whang, H. Lee, S.I. Jun, J. Oh, Y.J. Jeon, K. Kim, *Nature* 404 (2000) 982.

- [5] S. Wang, Z. Pang, K.D.L. Smith, M.J. Wagner, *J. Chem. Soc., Dalton Trans.* (1994) 955.
- [6] B. Barja, R. Baggio, M.T. Garland, P.F. Aramendia, O. Peña, M. Perec, *Inorg. Chim. Acta* 346 (2003) 187.
- [7] X. Li, X. Zheng, L. Jin, S. Lu, J. Zhang, *J. Mol. Struct.* 559 (2001) 341.
- [8] X. Li, L. Jin, S. Lu, J. Zhang, *J. Mol. Struct.* 604 (2002) 65.
- [9] A.W.H. Lam, W.T. Wong, S. Gao, G. Wen, X.X. Zhang, *Eur. J. Inorg. Chem.* (2003) 149.
- [10] C. Seward, N.X. Hu, S. Wang, *J. Chem. Soc., Dalton Trans.* (2001) 134.
- [11] X. Li, X. Zheng, L. Jin, S. Lu, W. Qin, *J. Mol. Struct.* 519 (2000) 85.
- [12] X. Li, L. Jin, X. Zhang, S. Lu, J. Zhang, *J. Mol. Struct.* 607 (2002) 59.
- [13] G.M. Sheldrick, *SHELX-97, Program for X-ray Crystal Structure Solution and Refinement*, Göttingen University, Germany, 1997.
- [14] J.H. Burns, W.H. Baldwin, *Inorg. Chem.* 16 (2) (1977) 289.
- [15] J.F. Ma, Z.S. Jin, J.Z. Ni, *Chin. J. Struct. Chem.* 10 (2) (1991) 125.
- [16] W. Brzyska, A. Kula, *J. Therm. Anal.* 34 (1988) 899.
- [17] H.Y. Zeng, Y.S. Yang, S.H. Huang, *Chin. J. Lumin.* 16 (4) (1995) 354.
- [18] M.C. Yin, L.J. Yuan, C.C. Ai, C.W. Wang, E.T. Yuan, J.T. Sun, *Polyhedron* 23 (2004) 529.
- [19] L.J. Yuan, M.C. Yin, E.T. Yuan, J.T. Sun, K.L. Zhang, *Inorg. Chim. Acta* 357 (2004) 89.
- [20] J.T. Sun, W. Xie, L.J. Yuan, K.L. Zhang, Q.Y. Wang, *Mater. Sci. Eng. B64* (1999) 157.
- [21] P.C.R. Soares-Santos, H.I.S. Nogueira, J. Rocha, V. Félix, M.G.B. Drew, R.A.S. Ferreira, L.D. Carlos, T. Trindade, *Polyhedron* 22 (2003) 3529.